PETROLEUM EXPLORATION WITH AIRBORNE RADAR (SAR) AND GEOLOGIC FIELD WORK, SINU BASIN OF NORTHWEST COLOMBIA*

James M. Ellis[1] and Larry L. Dekker[2]

[1]Chevron Overseas Petroleum Inc.
San Ramon, California, U.S.A.

[2]Chevron Niugini Pty. Ltd.
Port Moresby, Papua New Guinea

ABSTRACT

Stereoscopic, synthetic aperture radar (SAR) acquired over the cloudy Sinu Basin of Northwest Colombia in 1986 successfully: (1) mapped regional geologic structures and stratigraphy, (2) extrapolated detailed geology acquired during field work to surrounding structures, and (3) generated an excellent base map. Previously unmapped mud volcanoes, lithologic changes, unconformities, stratigraphic pinch-outs, and strike-slip faults were interpreted from the 1986 SAR imagery. Essential stratigraphic and structural data needed to upgrade SAR imagery from a regional to a local mapping tool were obtained by L. Dekker and others in river channels and quarries.

The SAR flight lines were oriented N-S (E-look) to enhance the dominant, WNW-directed thrust faults. The E-look direction complements a 1969 Westinghouse radar mosaic (real aperture data), which had predominantly S-look directions. The resulting orthogonal, radar-look directions enhance subtle fractures and faults, while minimizing radar shadow. Overlapping flight strips allowed photogrammetric determination of bedding attitudes (strikes, dips, and structural plunge). Interpretation of airborne radar was augmented by air photos and portions of a space-shuttle radar (SIR-A) orbital strip. The 1986 digital SAR data were reprocessed at Chevron to derive more geologic information.

1.0 INTRODUCTION

The Sinu Basin of Northwest Colombia (Figure 1) is of interest because of its extensive structural development, widespread hydrocarbon seeps (including mud volcanoes) and limited exploration. Chevron Overseas Petroleum Inc. was evaluating acreage in this basin and needed a regional mapping tool to: (1) understand the relationship between faults, mud volcanoes and stratigraphy, (2) map the regional outcrop pattern of resistant sandstones and conglomerates to improve understanding of the distribution of potential reservoir rocks, (3) map mud volcanoes and other hydrocarbon seeps, and (4) rapidly generate an accurate map base (Figure 2).

Multispectral satellite imagery (Landsat MSS and TM) of this basin has excessive cloud cover. Air photo mosaics have excellent resolution but significant planimetric distortions. Airborne radar imagery is available over much of the basin because in 1969 a survey was flown with real aperture radar (SLAR) by Westinghouse for the U.S. Army Engineer Topographic Laboratory (see Wing and MacDonald, 1973). This 1969 survey produced a 1:250,000 mosaic; however, it is uncontrolled and has significant areas geometrically distorted or in rain shadow.

In 1985, Chevron successfully utilized airborne SAR in cloudy Papua New Guinea for mapping structural geology in support of petroleum exploration (Ellis and Pruett, 1986). This data set was stereoscopic, digital, and it had 4 x 12 m pixels. Because of the exceptional structural information that was gleaned from this data, it was decided to acquire similar remote sensing imagery over the Sinu Basin.

17,000 km^2 was surveyed with SAR in two days during March 1986 (Figure 16). The northern half of the basin is farmed and relatively flat. The southern half is more rugged with relief to 1400 m. The area is dominated by shales and siltstones and is characterized by numerous mud volcanoes (see Duque Caro and others, 1983, Figure 3a). Outcrops are difficult to find in the field due to deep weathering, lush vegetation and extensive cultivation (Figure 3b). Geologic field data (strikes, dips, faults and stratigraphy) were largely collected in quarries and at occasional outcrops along river channels (Figure 3c-d).

2.0 SAR SURVEY DESIGN AND ACQUISITION

The new survey was flown N-S with an E-look direction to accentuate structures trending NNE-SSW and to complement the 1969 Westinghouse survey with its E-W flight lines and dominantly S-look. Topographic relief, cloud cover, and radar shadow increase toward the southern portion of the Sinu Basin with the rise of the Cordillera Occidental. A single-look direction flight strip over the high Cordillera would have excessively long shadows covering east-facing mountain flanks. No terrain information would be recorded by our SAR survey along these flanks. To overcome the loss of data due to shadow, the flight strip over the highest terrain was recorded with two-look directions (see Figure 10c and d).

Clouds covered 90% of the southern Sinu Basin during the survey. Cumulonimbus thunderheads commonly rose across the radar beam during acquisition. Twice radar shadows were cast by frozen moisture within these convectional cells. These flight strips were reflown. The northern portion of the Sinu Basin has an extensive rural population. Smoke from burning fields created a dense ground haze. Cumulus cloud cover averaged 40%. Radar successfully penetrated both haze and clouds.

Flight strip overlap averaged 55%. A total of nine strips with an E-look direction were acquired. These were mosaiced by hand to a UTM grid at a scale of 1:250,000, providing an excellent map base.

3.0 STRATIGRAPHY AND MUD VOLCANOES

The second author mapped the Rio Broqueles area (Figure 4a-d) in detail by traversing river channels during the dry season (January - April; see Figures 5a-d). The understanding of the stratigraphy of this area was critical to our exploration effort and previous geological maps were not comparable. Hundreds of field observations (dips, strikes, faults, and lithology) were made, which were extrapolated by interpretation of air photographs (Figure 4a). The resulting geologic map is highly detailed; a simplified version is depicted in Figure 4b. The unenhanced Landsat MSS image (Figure 4c) was of little value for geologic mapping due to poor resolution, uniform vegetation cover, and high sun angle.

The 1986 SAR survey complemented the field and air photo work and provided new geologic information in the Rio Broqueles area. It can be seen that SAR provides an exceptional image of relative rock competence across the entire area that can be directly related to lithogies mapped in the field (Figure 5a-d). In addition, due to the low illumination angle, SAR displays more bedding and faulting than the Landsat or photogeologic map.

Field work encountered numerous disturbed areas where exotic blocks were disoriented with respect to regional strike (Figure 4b). The geologists in the field and the air photo interpreters often interpreted these chaotic deposits as mud volcano deposits. However, after acquisition of the SAR imagery, it could be seen that **in situ** beds were often continuous through these zones. Interpretation of the SAR images suggested that these chaotic deposits were primary depositional features known as olistostromes (R. C. Crane, 1986, pers. comm.) that were created by submarine mass-wasting during deposition.

Mud volcanoes have a characteristic radar texture and typically exhibit radial drainage (Figure 6). Accurate mapping of mud volcanoes in relation to structural and stratigraphic trends was possible with the SAR data, and helped explain geochemical data collected at vents.

4.0 STRUCTURAL GEOLOGY

Within the Rio Broqueles area (Figure 4d) a set of beds can be delineated on the SAR image that appear to be large-scale cross beds that terminate in a local, angular unconformity. On the photogeological map the nature of these beds is not apparent due to a lack of detail. While interpreting the area immediately south of Rio Broqueles with SAR, similar units were mapped (Figure 7). Interpretation of the radar suggests that there is a major left-lateral, strike slip fault, trending WNW-ESE which offsets these units by about 17 km. A fault was mapped here previous to the SAR survey; however, it had a vertical sense of motion based on different ages north and south of this zone. Combining this field data and the SAR interpretation results in identifying an important wrench fault with significant vertical and horizontal motion.

"Rimmed synclines", such as the "Monitos" structure (Figure 8), dominate the central portion of the basin (Duque-Caro, 1979). On the 1969 radar survey this structure is apparent, but poorly defined (Figure 8a). Based on field work and air photo interpretation, outcrops were assigned geologic ages (Figure 8c). This detailed work is augmented by additional structural information available on the 1986 SAR image (Figure 8b). Mud volcanoes and their structural relationship to faults and margins of synclines are best displayed on the 1986 radar. The new radar also provides additional strike and dip information.

5.0 COMPARISON OF RADAR AND MULTISPECTRAL IMAGES

On the eastern margin of the basin, images from the 1969 and 1986 airborne radar surveys overlap with 1973 Landsat MSS and 1984 TM (Figure 1b). The area is partially covered with a 1:50,000-scale, uncontrolled air photo mosaic that contains the most detailed cultural information but has significant distortions. The 1969 real aperture radar mosaic has excellent detail; however, it suffers from internal geometric distortions that also precludes its use as a reliable map base (Figure 9a). The Landsat MSS image is cartographically superior, but it only displays major rivers and roads, and larger towns (Figure 9b). The 1986 synthetic aperture mosaic (Figure 9c) is a reliable map base and detail is outstanding. The color IR Landsat TM has excellent cultural information in flat terrain, but clouds cover hills (Figure 9d).

6.0 COMPARISON OF THREE RADAR SENSORS

In the southwestern corner of the surveyed area, airborne and spaceborne radar images overlap (Figure 1b). The terrain is flat in the western portion of this area and abruptly rises to the east of a major NNW-SSE trending fault. The 1969 radar displays a patchwork of flight lines (Figure 10a). The SIR-A image recorded by NASA's space shuttle was captured with a synthetic aperture system, was processed holographically, and has a 50 m resolution (see Sabins, 1983; Figure 10b). The SIR-A image is superior to the real aperture image, but it does not display a variety of textures in the Cordillera Occidental. The airborne SAR images (Figures 10c and 10d) accentuate structure and clearly display different textures within the Cordillera; these represent different lithologies.

7.0 DIGITAL REPROCESSING

The 1986 radar data were acquired with a digital system in standard resolution (4 x 12 m pixels). To reduce the number of pixels in the data set, the contractor summed and averaged three pixels along track creating 12 x 12 m pixels. Even with this summation of data, a radar image of 12 km^2 of area is represented by 1,000,000 pixels.

Cliffs that faced the radar antenna, recent coastal deposits, and dry lake beds reflected, as expected, relatively large amounts of microwave energy resulting in excessively bright (oversaturated) zones on the original flight strips. Contrast stretching and color-density slices were found to be the most useful digital enhancement techniques to bring out new information.

8.0 REFERENCES

Duque-Caro, H. 1979, Major structural elements and evolution of Northwestern Colombia: American Association of Petroleum Geologists Memoir 29, p. 329-351.

Duque-Caro, H., W. D. Page, and J. Cuellar, 1983, General geology, geomorphology, and neotectonics of northwestern Colombia: 10th Caribbean Geological Conference, Field Trip C, Cartagena, August 20-24, 1983, 62 p.

Ellis, J. M. and F. D. Pruett, 1986 - Application of Synthetic Aperture Radar (SAR) to Southern Papua New Guinea Fold Belt Exploration: Proceedings of the Fifth Thematic Conference on Remote Sensing for Exploration Geology; Reno, Nevada (ERIM), p. 15-34.

Sabins, F. F., 1983, Geologic interpretation of space shuttle radar images of Indonesia: American Asssociation of Petroleum Geologists Bulletin, v. 67, no. 11, p. 2076-2099.

Wing, R. S. and H. C. MacDonald, 1973, Radar geology-petroleum exploration technique, Eastern Panama and Northwestern Colombia: American Association of Petroleum Geologists Bulletin, v. 57, no. 5, p. 825-840.

9.0 ACKNOWLEDGMENTS

We thank Chevron Overseas Petroleum Inc. and ECOPETROL (Colombia's National Oil Company) for permission to publish this paper. The SAR images were acquired by Intera Technologies, Ltd. The mosaic was constructed by Mars Associates. T. G. Osborn (Intera) and R. H. Gelnett (Mars) were particularly helpful.

The field work was supported by excellent air photographic interpretation and mapping by GEOTEC LTDA. of Bogota, Colombia. Carlos Caceres' work is acknowledged. Chevron Oil Company of Colombia (G. Perez and C. Hartmann) was instrumental in expediting the SAR acquisition and in assisting L. Dekker's two-year field effort. Discussions with F. A. Lindberg and S. R. Winter of Chevron were very helpful.

F. F. Sabins, W. S. Kowalik, and T. F. Battey of Chevron Oil Field Research Company assisted in reprocessing the data. F. F. Sabins also helped plan the survey. ECOPETROL geologists helped interpret the radar data. Portions of this paper were presented to and benefited from the 1987 Latin-American Conference on Remote Sensing and the Colombian Association of Geologists and Geophysicists in Bogota. Photographic copies of the 1969 radar mosaic and the 1986 radar flight strips and mosaic are on file at Instituto Geographico 'Agustin Codazzi', Bogota.

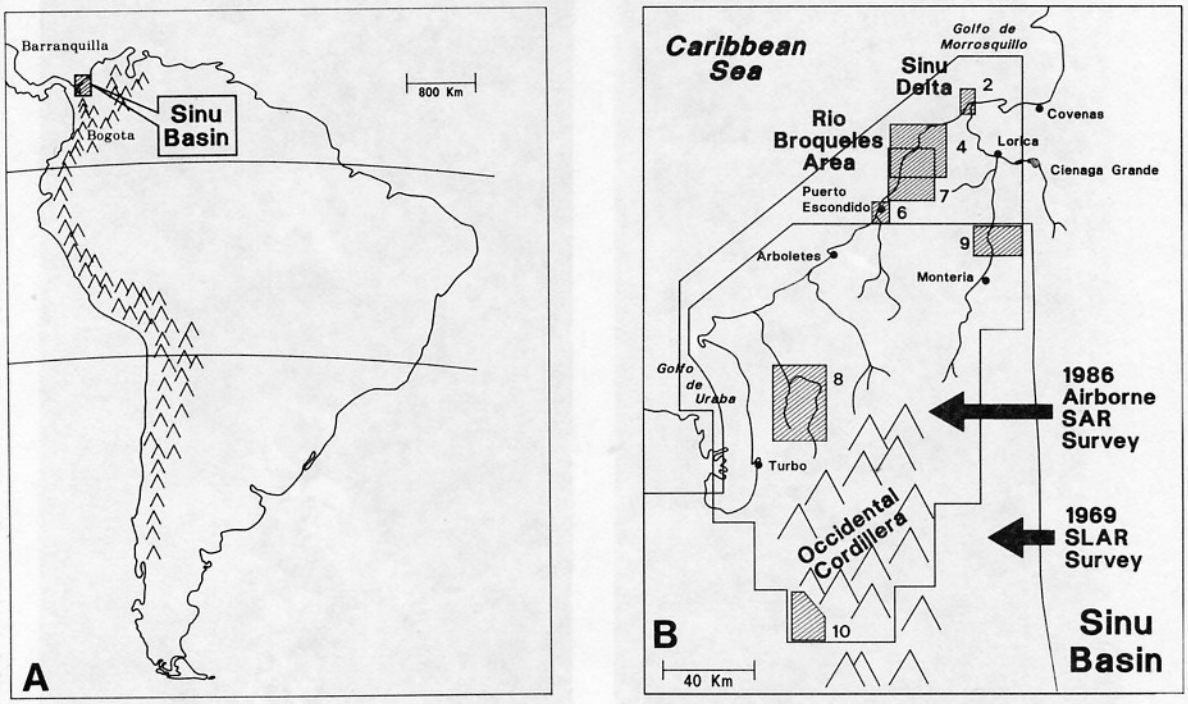

1 A) Location map of Sinu Basin, NW Colombia. B) Sinu Basin with outlines of 1969 and 1986 airborne radar surveys and locations of Figures 2, 4, 6, 7-10.

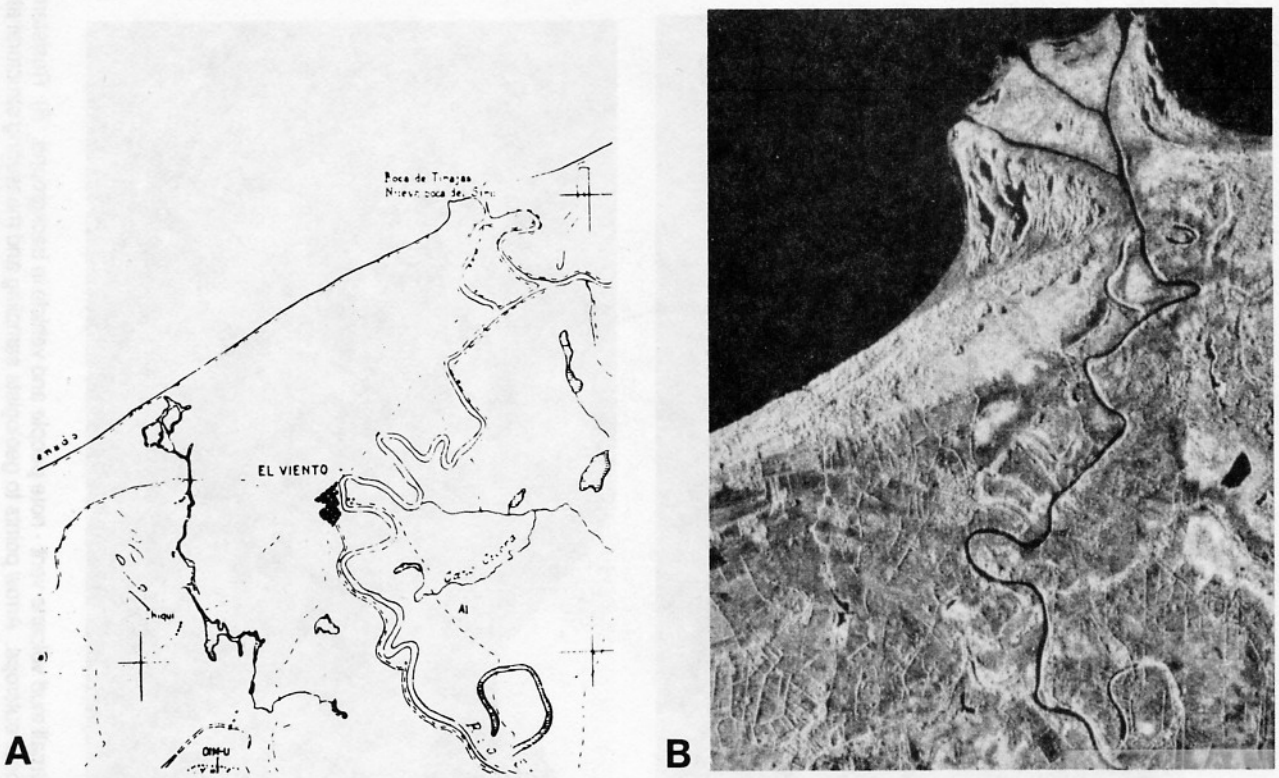

2) Comparison of map (A) generated from air photographs acquired in the 1950's (?) (van der Harst and Maurenbrecher, 1959) with same-scale, 1986 airborne SAR image (B). Over 3 decades a new delta was deposited and the Sinu River changed course (see El Viento). SAR image (B) of delta reveals excellent textural detail related to geomorphology and grain size of sediments. Scale about 1:140,000.

A

B

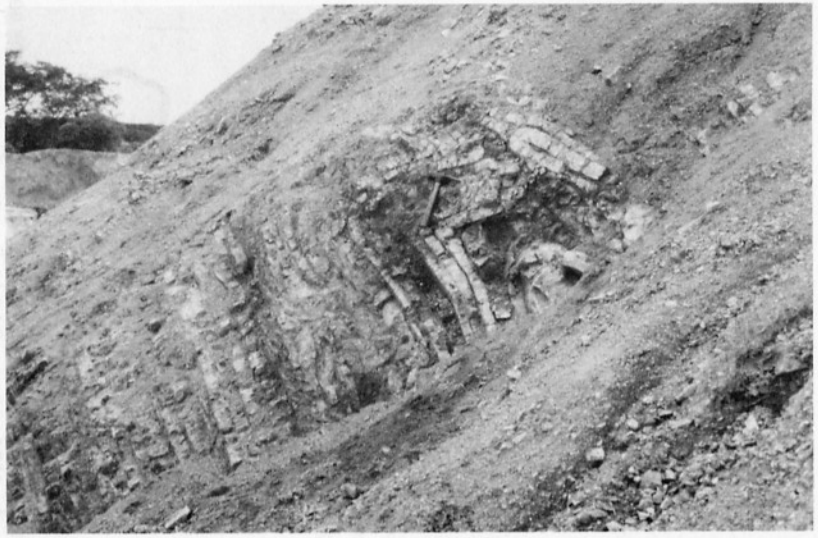

C

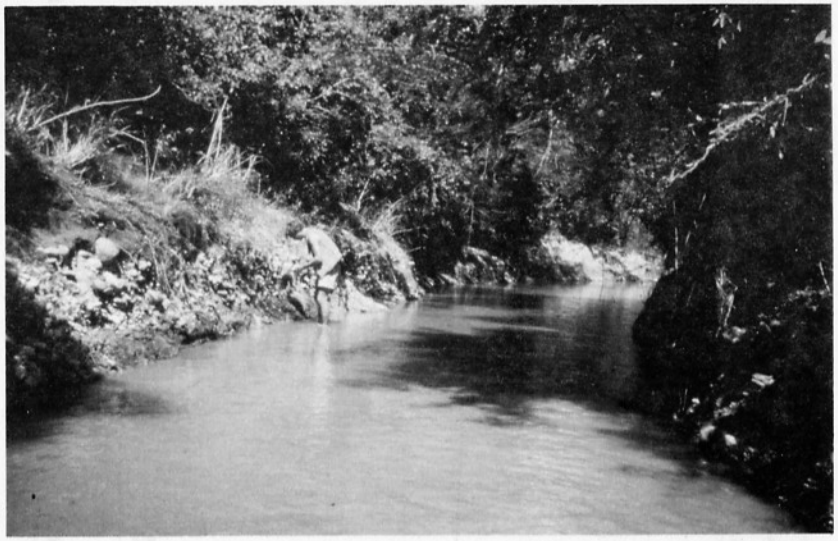

D

3A) Small mud volcano vent - note people and vehicle in background. B) Resistant ridge of Manantial sandstone showing typical extensive cultivation, soil development, and poor outcrops. Arrow points to geologists sampling and measuring structural attitude of small outcrop near base of ridge. C) Folded beds as revealed in quarry near Monteria. D) L. Dekker at typical sampling site along stream channel.

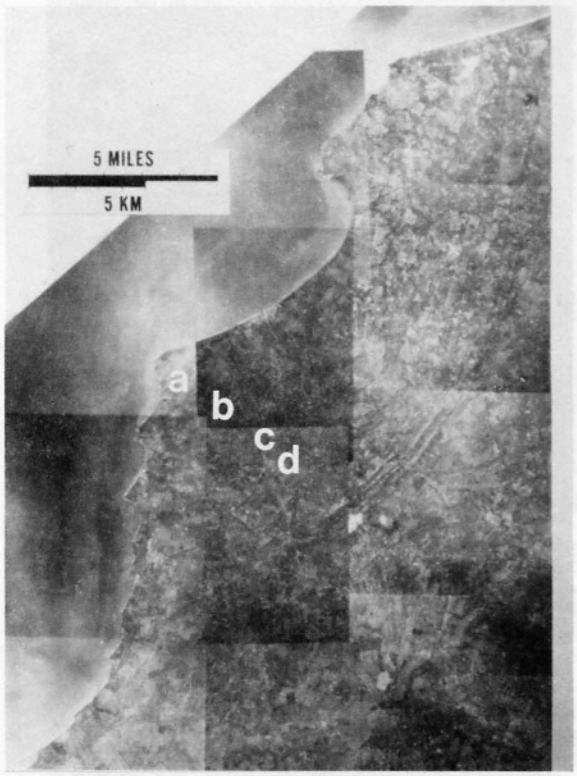

A

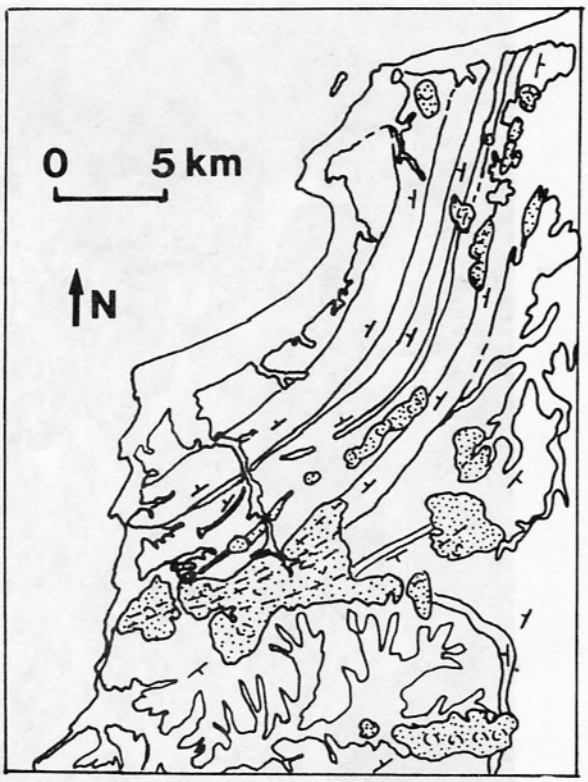

B

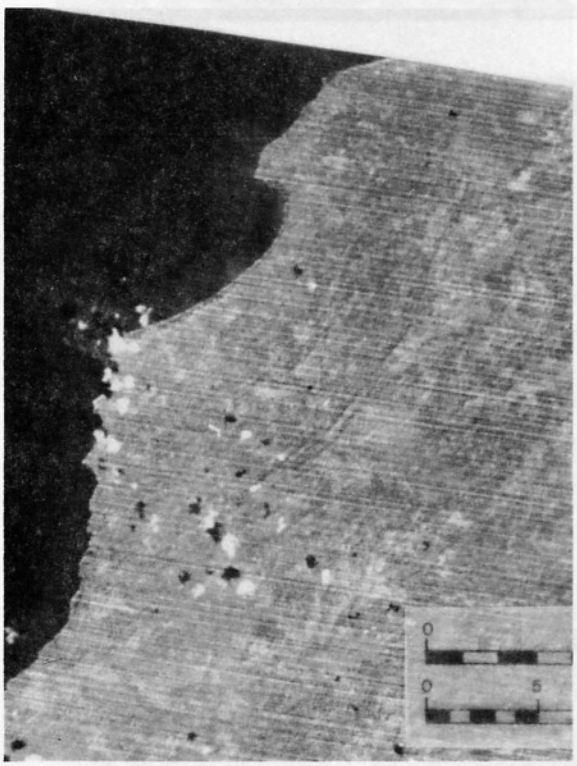

C

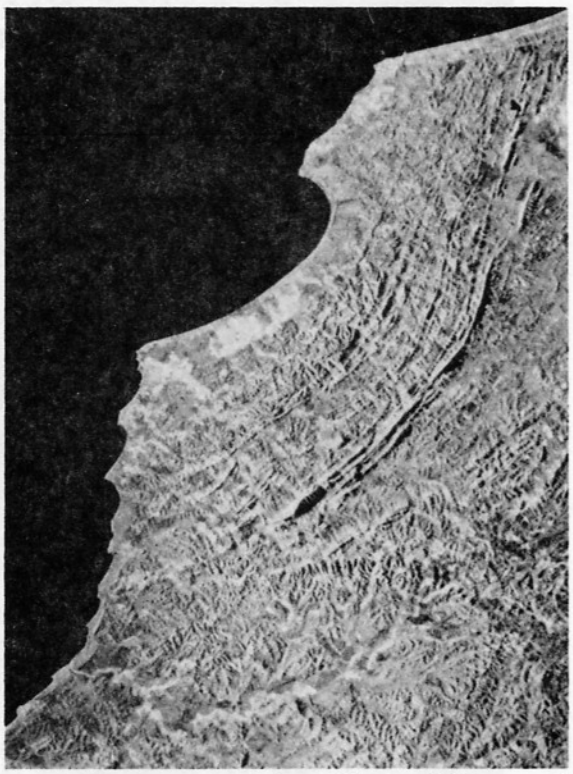

4) Rio Broqueles area depicted with same-scale (A) air photo mosaic (letters a-d refer to locations of Figures 5A-D, respectively), (B) simplified photogeologic map that included field data, (C) unenhanced Landsat MSS image, and (D) 1986 SAR image. On map, dotted areas were interpreted on air photos and field work to be mud volcanoes and/or zones of chaotic deposits. Scale about 1:300,000.

A

B

C

D

5) Field photographs of Rio Broqueles area (see Figure 4A for locations and Figure 4D for lithologic comparisons. (A) Incompetent claystones of a shale unit - flat terrain, outcrop mostly covered by vegetation, (B) slightly more competent shale unit with coarse-nodular development, (C) massive siltstones with hard, concretionary beds that support competent ridges, and (D) interbedded sandstones and shales (with hard limestone beds) that also form resistant ridges.

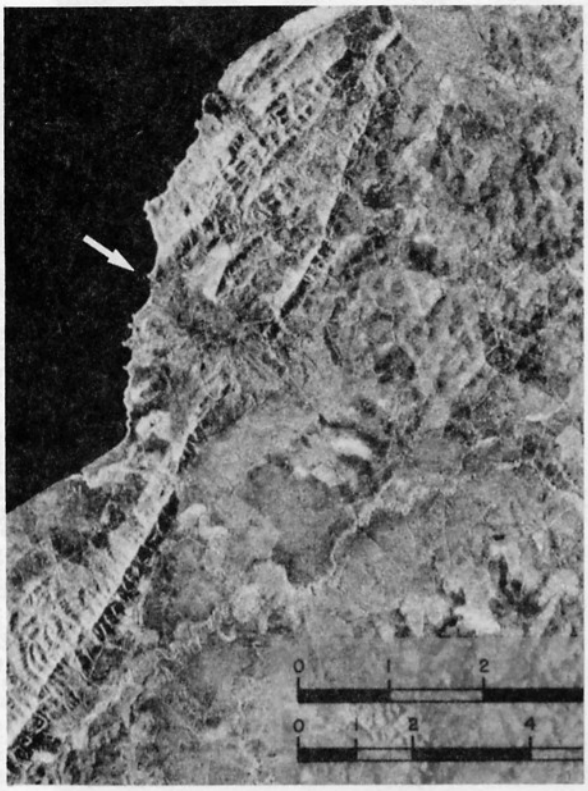

6) Mud volcano at Puerto Escondido (scale 1:125,000; see Duque-Caro and others, 1983 for recent history). Note NNE-SSW trending ridge that is buried under the east flank of the volcano. With SAR a thrust fault is interpreted along the west side of this linear ridge. The volcano is being formed by mobile shales that are moving along this fault toward the surface.

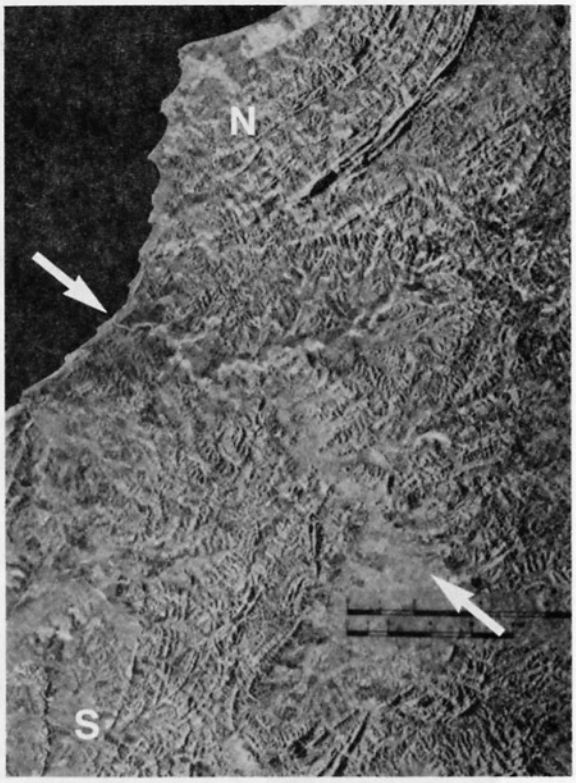

7) SAR image immediately south of Rio Broqueles area (see Figure 4D, scale about 1:300,000), showing new evidence for significant left-lateral, strike-slip movement. Outcrop patterns at "N" and "S" were interpreted to be the same geologic unit based on SAR. Fault zone is between arrows.

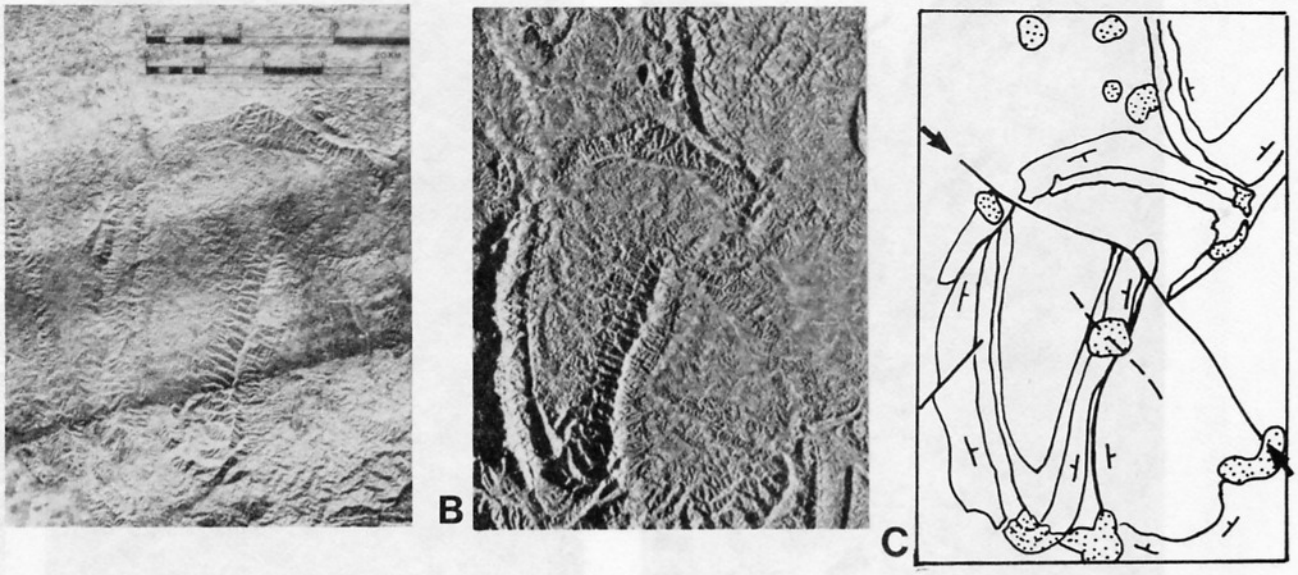

8) Comparison of same-scale (about 1:600,000) radar and map of Monitos rimmed syncline structure in central Sinu Basin. (A) 1969 radar, (B) 1986 airborne radar, and (C) simplified version of photogeologic map. ENE-WSW trending lines in (A) are mosaiced edges of individual flight strips. On map (C), arrows point to trace of significant strike-slip fault and dotted areas are mud volcanoes and/or chaotic zones (interpreted from air photos).

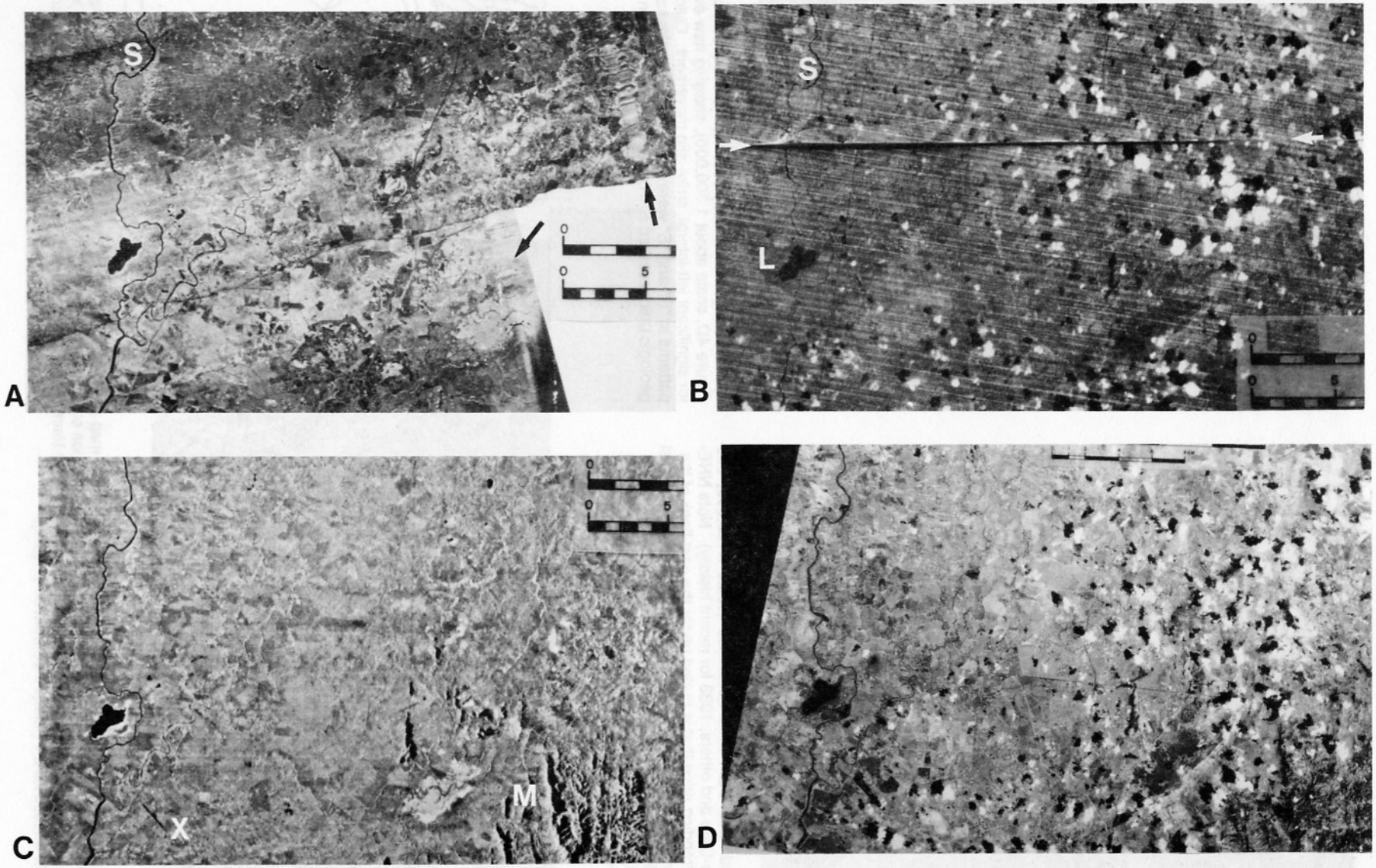

9) Comparison of same-scale (about 1:330,000) radar and Landsat in relatively flat terrain. "L" is lake, "S" is Sinu River, "X" is airport, and "M" is hilly terrain. (A) 1969 radar has good detail but significant geometric distortions along Sinu River and recording noise (see arrows). (B) 1973 unenhanced Landsat MSS shows little detail, every 6th scan line, and the seam between overlapping scenes (see arrows). (C) 1986 SAR has excellent detail and clearly images hills. (D) Landsat TM has excellent cultural information, but "popcorn" clouds obscure hills and some of flat terrain.

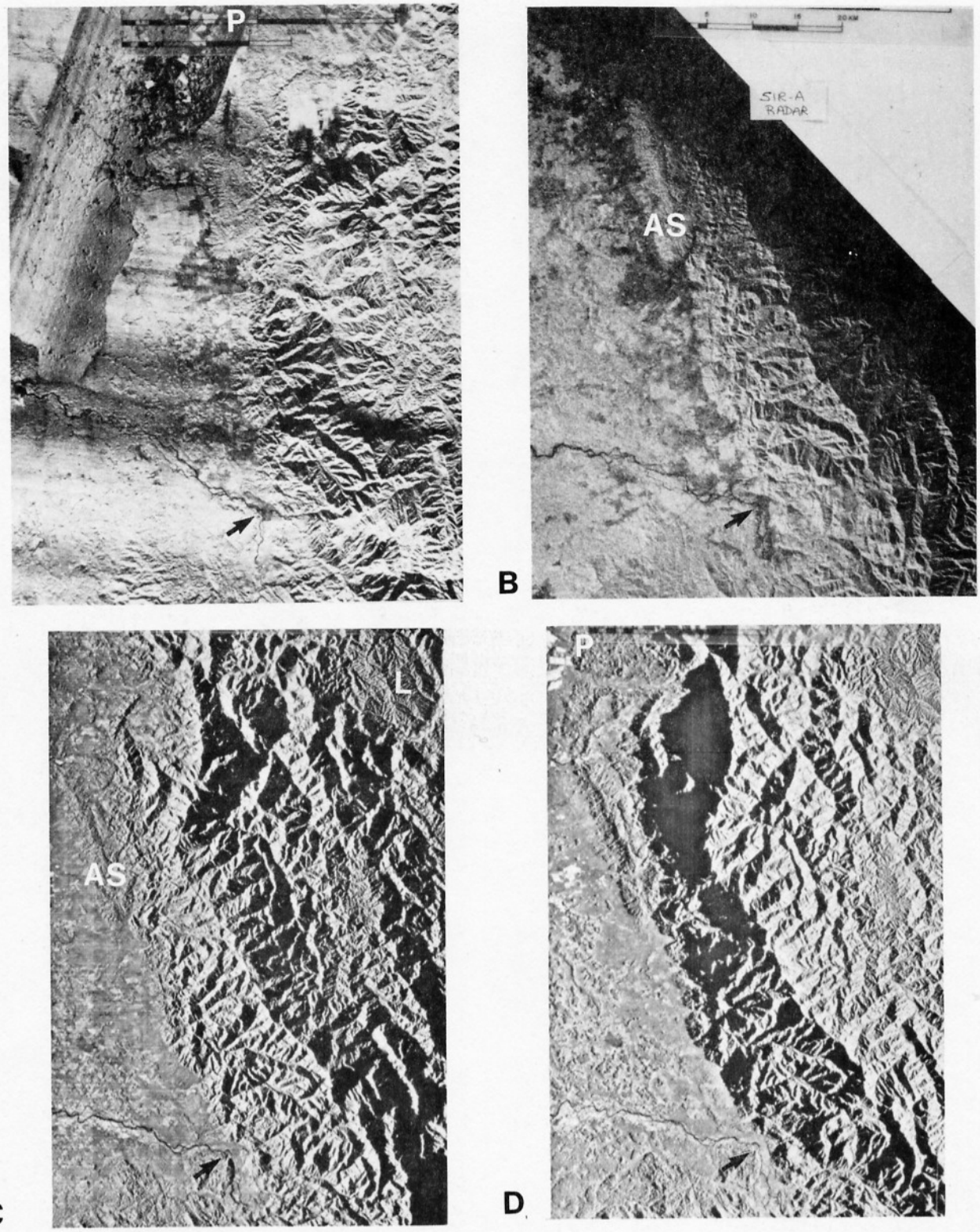

10) Same-scale comparison (about 1:625,000) of airborne and spaceborne radar in flat and mountainous terrain. "AS" is anticlinal structure, "L" is interpreted to be a distinct lithologic unit, "R" are radar shodows caused by moisture in cumulonimbus clouds, "P" are banana plantations, and arrows point to same location along river. (A) 1969 radar showing NNE-SSW oriented flight strip patched into mosaic, high reflectivity of banana leaves, and geometric distortions. (B) Far-range portion of SIR-A orbital strip (excessive shadow) showing subtle structures in southern lowlands and suggestion of "AS". (C) E-look1986 SAR showing pronounced structure at "AS" and unique radar texture at "L". (D) W-look 1986 SAR emphasizing "AS" due to increased shadowing in the far range of the flight strip.